Boston Scientific
Advancing science for life™

HeartLogic™
Heart Failure Diagnostic

SOME TECHNOLOGY IS GAME CHANGING.

THIS IS CAREER DEFINING.

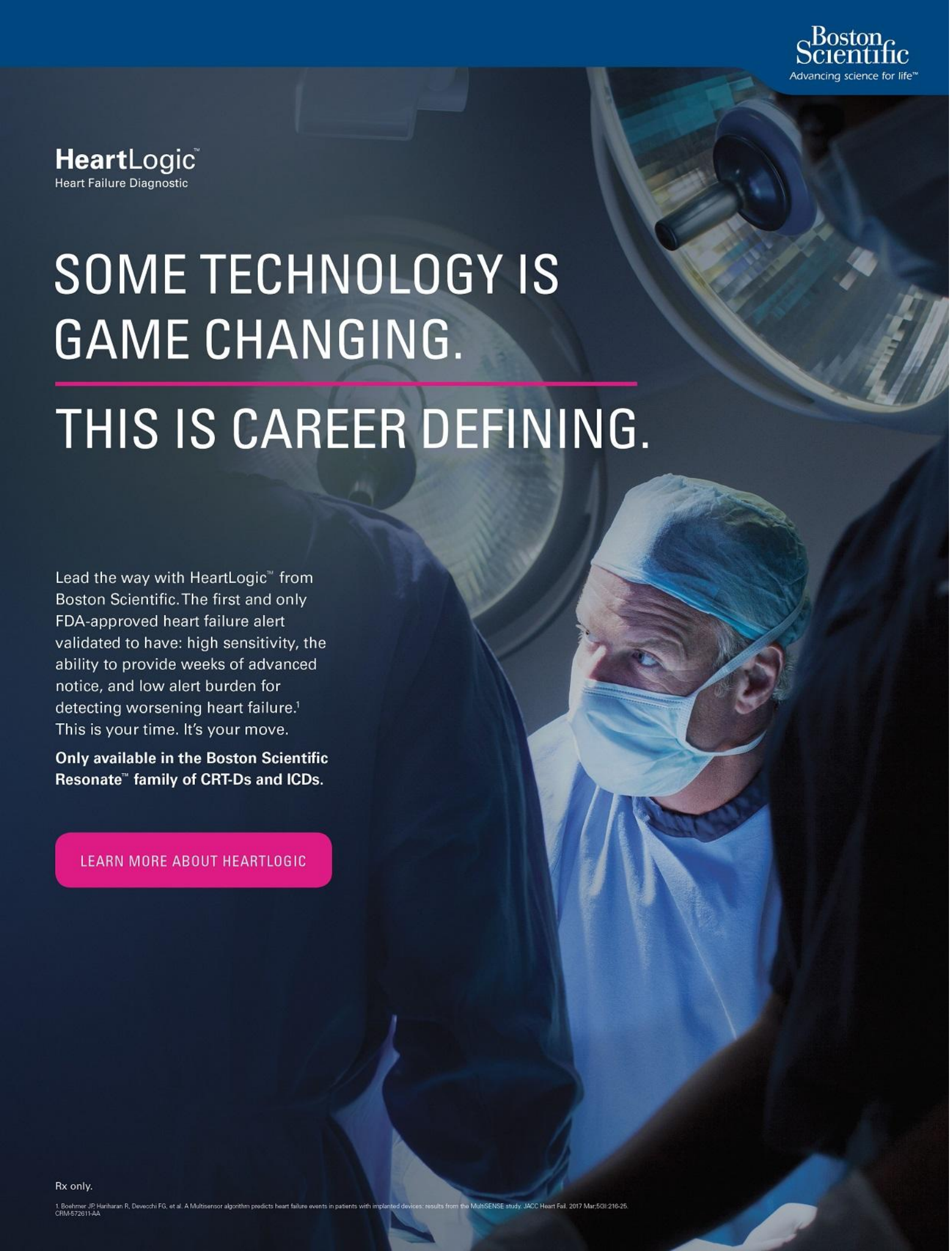

Lead the way with HeartLogic™ from Boston Scientific. The first and only FDA-approved heart failure alert validated to have: high sensitivity, the ability to provide weeks of advanced notice, and low alert burden for detecting worsening heart failure.[1] This is your time. It's your move.

Only available in the Boston Scientific Resonate™ family of CRT-Ds and ICDs.

LEARN MORE ABOUT HEARTLOGIC

Rx only.

1. Boehmer JP, Hariharan R, Devecchi FG, et al. A Multisensor algorithm predicts heart failure events in patients with implanted devices: results from the MultiSENSE study. JACC Heart Fail. 2017 Mar;5(3):216-25.
CRM-572611-AA

Interatrial Electrical Connections: The Precise Location and Preferential Conduction

SHUN-ICHIRO SAKAMOTO, M.D., TAKASHI NITTA, M.D., YOSUKE ISHII, M.D., YASUO MIYAGI, M.D., HIROYA OHMORI, M.D., and KAZUO SHIMIZU, M.D.

From the Department of Cardiothoracic Surgery, Nippon Medical School, Tokyo, Japan

Interatrial Electrical Connections. ***Background:*** **The atria are assumed to be connected electrically to each other at the level of the Bachmann's bundle, coronary sinus (CS) musculature, and interatrial septum, and these connections may have an important role in the interatrial conduction and perpetuation of various types of atrial tachyarrhythmias. However, the number, location, and preferential connections of the interatrial conduction related to the site of activation have not been examined yet.**

Methods: **The endocardium of both atria and the CS were mapped during continuous pacing from the left superior and inferior pulmonary veins, right pulmonary veins, upper and lower right atrium, or right atrial septum at various paced cycle lengths in 14 canines. The electrograms were recorded by custom-made form-fitted electrodes mounted on a specially designed device that allowed the septal aspects of the electrode forms to be spatially fixed to each other accurately.**

Results: **Four distinct interatrial electrical connections were identified at the Bachmann's bundle, CS, and antero-superior and postero-inferior septa. Decremental conduction was not seen in any of the connections. Bachmann's bundle was the most preferential connection during pacing from any epicardial site. The transseptal connections were evident only during pacing from the interatrial septum. The preference among the four connections was determined by the site of stimulation and the propagation of the activation related to the myocardial architecture.**

Conclusion: **These unique preferential connections may play a significant role in the interatrial conduction and perpetuation of atrial tachyarrhythmias.** *(J Cardiovasc Electrophysiol, Vol. 16, pp. 1077-1086, October 2005)*

interatrial conduction, atrial tachyarrhythmias, transseptal connection

Introduction

Since Bachmann proposed the anterior interatrial band as the primary connection between the right and left atria,[1] many studies have been performed to examine the interatrial electrical connections with regard to the histological and electrophysiological characteristics of the connections. Bachmann's bundle[1,2] and the coronary sinus (CS) musculature[3,4] have been demonstrated as the major interatrial connections, however, the number and precise location of the transseptal interatrial connections remain unclear. Further, the preference of the connections related to the site of origin of the activation and the activation sequence in the opposite atrium have not been examined in detail.

Small interatrial bundles are frequently recognized morphologically alongside Bachmann's bundle and presumed to be the antero-superior septal interatrial connection in humans.[5] An electroanatomic mapping study[6] distinguished the antero-superior septal connection from Bachmann's bundle during distal CS pacing in a few patients. Since the endocardial insertion of these connections to the right and left atria are adjacent to each other, a small difference in the site of origin of the activation or in the direction of the activation in the septum can affect the preference of the interatrial connection and the activation sequence in the opposite atrium.

The muscular bridges, joining the LA to the lower intercaval area on the RA and to the inferior vena cava, are presumed to be the postero-inferior interatrial connection.[7,8] The electrophysiologic study on the postero-inferior connection in humans is scarce. A canine study[9] using basket catheters placed in both atria demonstrated the interatrial conduction through the postero-inferior septal connection during pacing from the inferior RA septum. Another canine study[10] of epicardial and endocardial simultaneous mapping using high-resolution electrodes also demonstrated the posterior septal transmission between the LA and RA during stimulation of the posterior LA in the region of the pulmonary veins and the posterior RA endocardium. However, the precise location of the connection remains unclear, because the potentials in the right and left atrial septa were recorded by electrodes mounted on separate balloons that were inserted through small atriotomies and inflated transiently, and the potentials in the CS were not recorded in the study.

The aim of the study was to determine the precise location of the interatrial electrical connections and preferential connection related to the pacing site, particularly the pulmonary veins. We used a three-dimensional mapping system with an accurate fixation of the septal aspect of the custom-made endocardial electrodes in order to accurately examine the activation sequence of the intact right and left atria spatially.

Presented at the 23rd NASPE meeting, May 2002 and the 75th AHA meeting, November 2002.

Manuscript received 19 September 2004; Revised manuscript received 18 January 2005; Accepted for publication 3 March 2005.

Address for correspondence: Shun-ichiro Sakamoto, M.D., Cardiothoracic Surgery, Nippon Medical School, 1-1-5 Sendagi, Bunkyo-ku, Tokyo 1138603, Japan. Fax: 81-3-5685-0985; E-mail: saka-165@nms.ac.jp

doi: 10.1111/j.1540-8167.2005.40659.x

Methods

Animal Preparation

All animals received humane care in compliance with the "Principles of Laboratory Animal Care" formulated by the National Society for Medical Research and the "Guide for the Care and Use of Laboratory Animals" prepared by the National Academy of Science and published by the National Institute of Health (NIH Publication 86-23, received 1985). In addition, this study protocol was approved by the Animal Ethics Committee of Nippon Medical School.

Fourteen mongrel dogs of either sex (weight range, 25–30 kg) were subjected to the study. Anesthesia was induced with intravenous pentbarbital sodium (30 mg/kg). The animals were intubated endotracheally and ventilated using a volume limited ventilator. The limb-lead electrocardiograms and systemic arterial pressure were monitored continuously. The chest was opened via a median sternotomy. The pericardium was opened and the heart was suspended in a pericardial cradle. The azygos vein was divided. After systemic heparinization (2 mg/kg), a 12 Fr aortic cannula was inserted into the ascending aorta and a pair of 24 Fr venous cannuli were inserted into the superior and inferior vena cavae. Then, a normothermic total cardiopulmonary bypass was initiated with crystalloid solution. Arterial blood samples were drawn every 30 minutes to determine the arterial oxygen tension, acid–base balance, and electrolyte levels. These values were maintained within a physiologic level throughout each study.

Atrial Endocardial Electrodes and Coronary Sinus Catheter Electrode Placement

The endocardial atrial electrode forms were made of a silicon elastomer (Dow Corning Corp., Midland, MI, USA) and were constructed from molds contoured from postmortem, formalin-fixed canine atria. A total of 98 and 106 bipolar electrodes were distributed on the right and left atrial electrode forms, respectively (Fig. 1A). The electrodes were constructed from fine silver wire of 0.5 mm in diameter (Pacific Wire & Cable, Santa Ana, CA, USA) which was passed through the silicon electrode forms. Each bipolar electrode consisted of two silver-wire contact points located 1 mm apart with an interelectrode distance of 3 to 5 mm. Under a total cardiopulmonary bypass, bilateral ventriculotomies were performed and the mitral and tricuspid valve leaflets were excised. A CS catheter carrying 10 bipolar electrodes was inserted into the CS through a small hole corresponding to the CS ostium in the RA electrode form, subsequently the electrode forms were inserted into both intact atria through the ventriculotomies across the atrioventriuclar annuli retrogradely (Fig. 1B). Using a specially designed device to prevent horizontal and vertical wobbling, the interatrial septum was sandwiched firmly in place at the same electrode

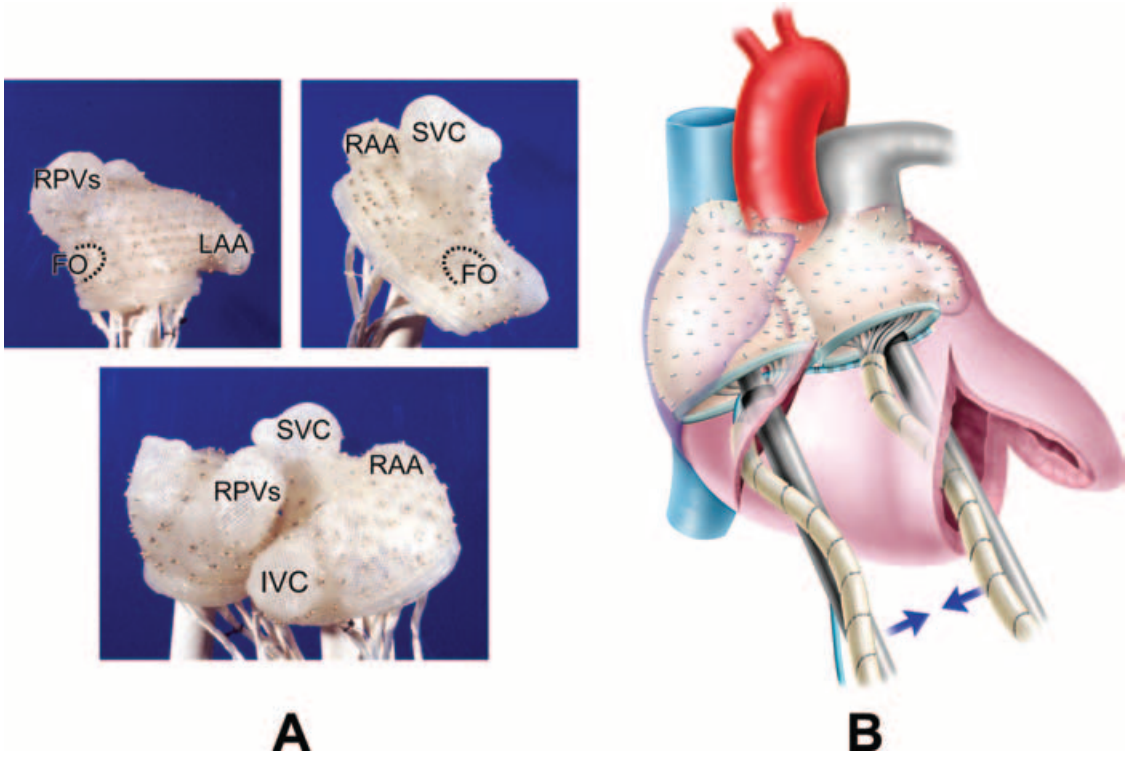

Figure 1. *A: Atrial electrode forms used in the study. The left and right upper panels represent the septal aspects of the left and right atrial electrode forms, respectively. The dotted line represents the corresponding site of the fossa ovalis in each aspect of the septum. A total of 98 and 106 bipolar electrodes were distributed on the right and left atrial electrode forms, respectively. The lower panel represents the postero-inferior view of the two electrode forms, showing the spatial correlation of the forms. B: The electrode forms and a CS catheter were inserted into the right and left atria through the bilateral ventriculotomies across the atrioventricular annuli retrogradely while the animal was perfused by a normothermic cardiopulmonary bypass. The septal aspects of the electrode forms were accurately positioned by holding the forms with rods that were spatially fixed to each other. RPVs = right pulmonary veins; LAA = left atrial appendage; RAA = right atrial appendage; SVC = superior vena cave; IVC = inferior vena cave; FO = fossa ovalis.*

location regardless of the thickness and shape of the septum in each study.

Stimulation

Electrical stimulation was performed using a programmable pulse generator (Cardiac Stimulator, FUKUDA DENSHI Corp., Tokyo). Continuous pacing was conducted at a cycle length from 350 to 200 msec in 50 msec decrements, and from 200 msec to the local effective refractory period in 10 msec decrements. The pacing output was set at twice the diastolic threshold. During pacing from the interatrial septum, the pacing output was decreased as low as possible to prevent far field stimulation of the contralateral side of the septum.

In nine animals, a custom-made hook-type bipolar pacing electrode was placed on the epicardium of the higher RA, lower RA (LRA), left superior pulmonary vein (LSPV), and left inferior pulmonary vein. In five canines, the right pulmonary veins (RPVs) were paced endocardially at the ostium of the veins after removing the LA electrode form, because epicardial pacing of the RPVs was not feasible due to the presence of the RA electrode form. The sites of the epicardial stimulation are indicated in Figure 2.

In five animals, the RA electrode form was removed, leaving the CS catheter and the LA electrode form, and then stimulation was performed from the inferior septum (anterior to the Tendon of Todaro), mid-septum (anterior limbus of the fossa ovalis), and superior septum. In three canines, stimulation was performed also from the posterior septum (posterior limbus of the fossa ovalis). The sites of the endocardial stimulation are indicated in Figure 3.

Data Acquisition and Analysis

A 256-channel mapping system that allowed simultaneous recording of up to 256 signals was used for the data acquisition and analysis. The system is based on a high-performance graphics workstation (Indigo 2, Silicon Graphics Inc., Mountain View, CA, USA). The system is run with custom-made software that was developed in the cardiothoracic surgery research laboratory in St. Louis, MO, USA and is capable of data acquisition control, management, display, and analysis. A limb-lead electrocardiogram was simultaneously

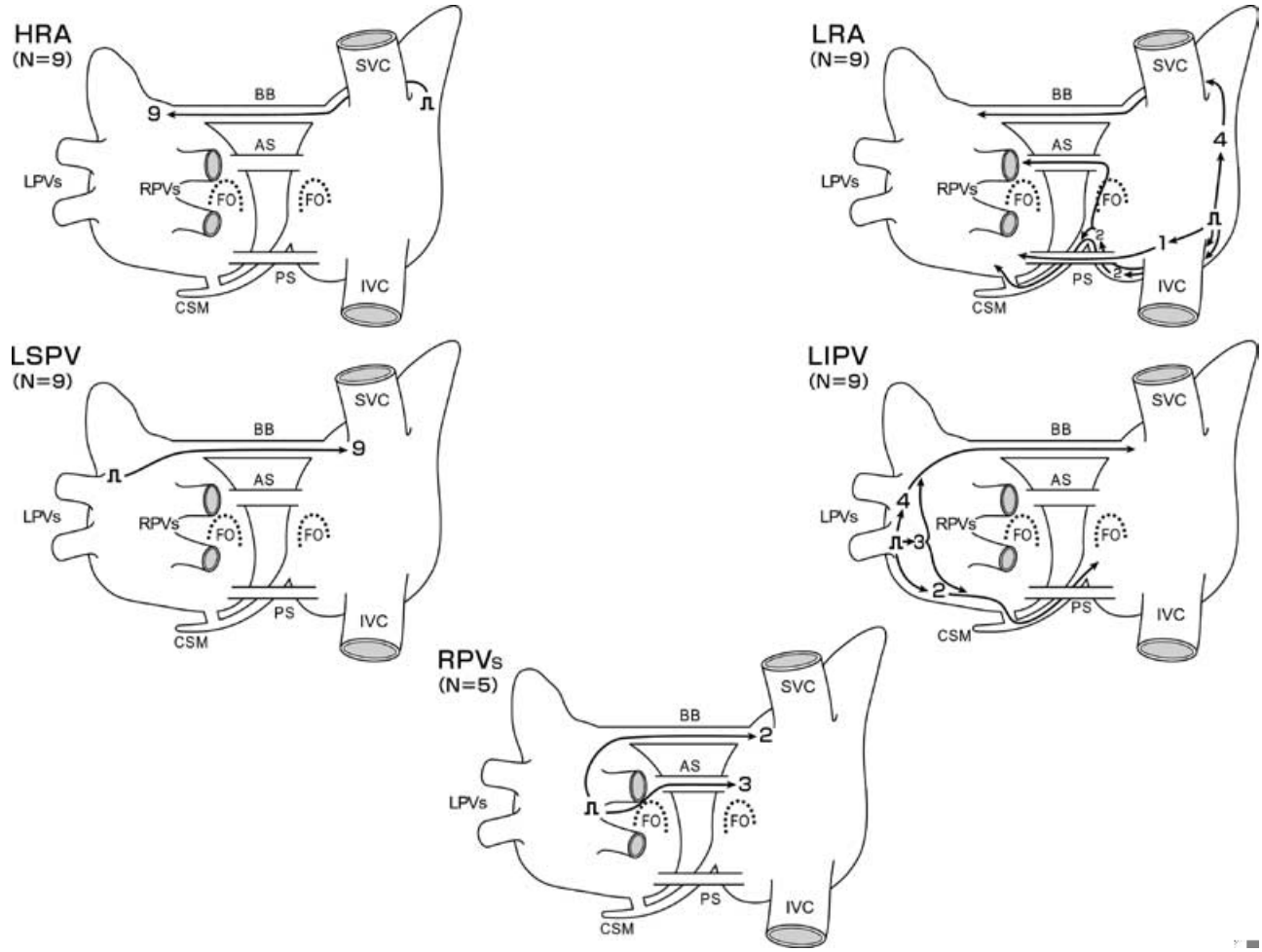

Figure 2. *Patterns of the preferential connections during pacing from the epicardium (n = 9) of the HRA, LRA, LSPV, LIPV, and endocardium of the ostium of the RPVs (n = 5). The schematic diagrams represent the right and left atria viewed posteriorly with the four distinct interatrial connections: BB, AS, PS, and CSM. The rectangle indicates the site of stimulation. The arrows indicate the interatrial preferential connection for each pacing site. Each number represents the number of animals, in which the connection was demonstrated as the preferential interatrial connection. BB = Bachmann's bundle; AS = anterior septum; PS = posterior septum; CSM = coronary sinus musculature; FO = fossa ovalis; LPVs = left pulmonary veins; HRA = high right atrium; LRA = low right atrium; LSPV = left superior pulmonary vein; LIPV = left inferior pulmonary vein.*

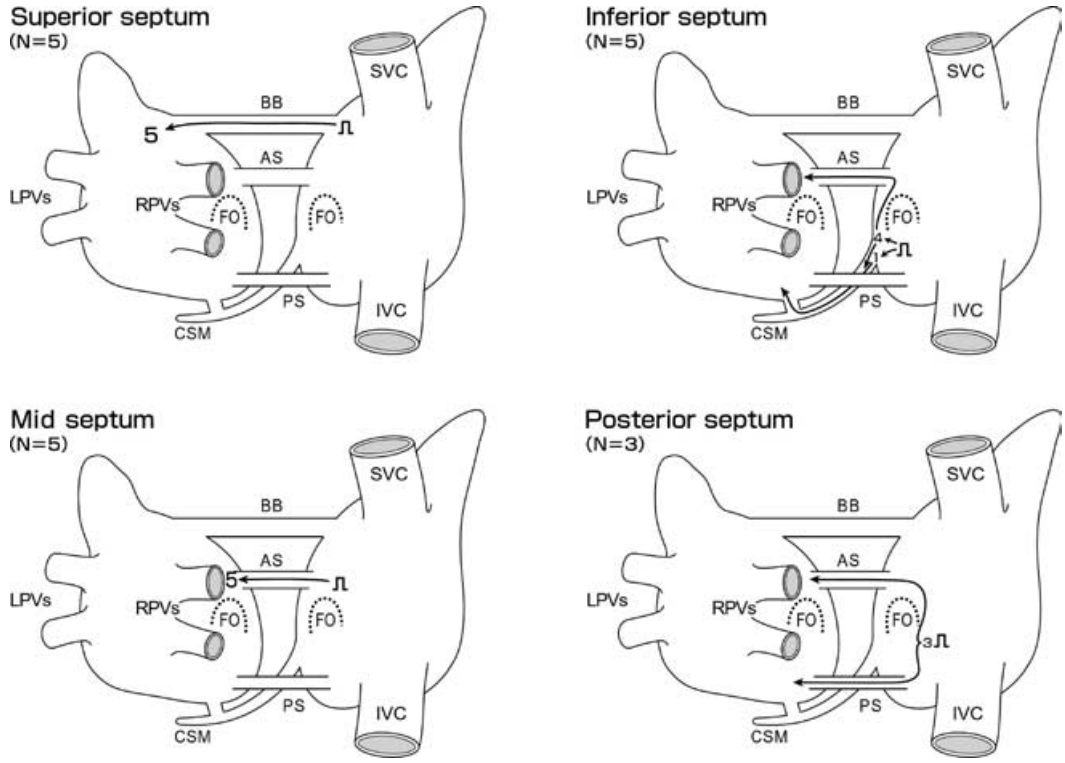

Figure 3. *Patterns of the preferential connections during pacing from the right-sided endocardim of the superior, inferior, and mid-septum (n = 5), as well as from the posterior septum (n = 3). The schematic diagram and figure symbols are the same as in Figure 2.*

recorded. Data were recorded during continuous pacing as described above. Bipolar electrograms were recorded at a gain of 250 with a frequency response of 5 to 500 Hz. Each channel was digitized at 2000 Hz with a 12-bit resolution. The local activation time was defined as the time of the maximum absolute amplitude of the bipolar electrograms. Activation maps were displayed on three-dimensional constructed models on a computer. The three-dimensional atrial models were constructed from the scanned images of cross sections of the cadaver atria of a canine. Rotation could occur in any combination of the x, y, or z axis. In addition, right or left atrial endocardial surfaces could be differentially made invisible.

Preferential connections were defined as connections that activated any extent of the contralateral atrium. An activation blocked in the CS was not considered as a preferential connection. The location of the interatrial connections was defined as the earliest activation site on the endocardium in the contralateral atrium. More than one preferential connection was considered present when more than one early activations appeared and the activation wavefronts collided with each other. After the experiment, the animal was euthanized and the atria were excised with the electrode forms attached. The accurate location of the electrodes in the septum was verified by marking them in relation to the anatomical landmarks in each animal.

The conduction properties of each interatrial connection were examined in all animals. Since the proximal end of the connection could not be localized precisely by the activation maps, the activation time at the earliest endocardial activation sites in the contralateral atrium was determined for each pacing cycle length, to examine the conduction property in each connection. Then the activation time difference was plotted as a function of the pacing cycle length.

Results

Interatrial Electrical Connections During Epicardial Pacing

The patterns of preferential interatrial connections during pacing from each epicardial site are illustrated in Figure 2. Bachmann's bundle was the most preferential connection during pacing from most of the epicardial sites. During pacing from the higher RA, the earliest breakthrough in the LA appeared in the endocardium of the superior LA, which corresponded to one end of Bachmann's bundle, in all animals. After the activation reached the superior LA, the activation propagated inferiorly over the left-sided interatrial septum and posterior LA (Fig. 4).

The preference of the interatrial connection was inconsistent during pacing from the LRA. Bachmann's bundle was the preferential connection in four animals, while in five animals, the activation did not conduct over Bachmann's bundle, but over other electrical connections, such as the CS musculature or anterior or posterior septal connections. In two animals, the stimulated activation propagated both over the anterior septal connection and the CS musculature, resulting in two distinct breakthrough sites in the LA: the anterior septum and the posterior LA (Fig. 5). Two wavefronts from the breakthrough sites collided with each other at the inferior LA (site d in Fig. 5A). In two animals, the CS musculature was the single preferential connection during pacing from the LRA. In one animal, the earliest breakthrough was identified at the

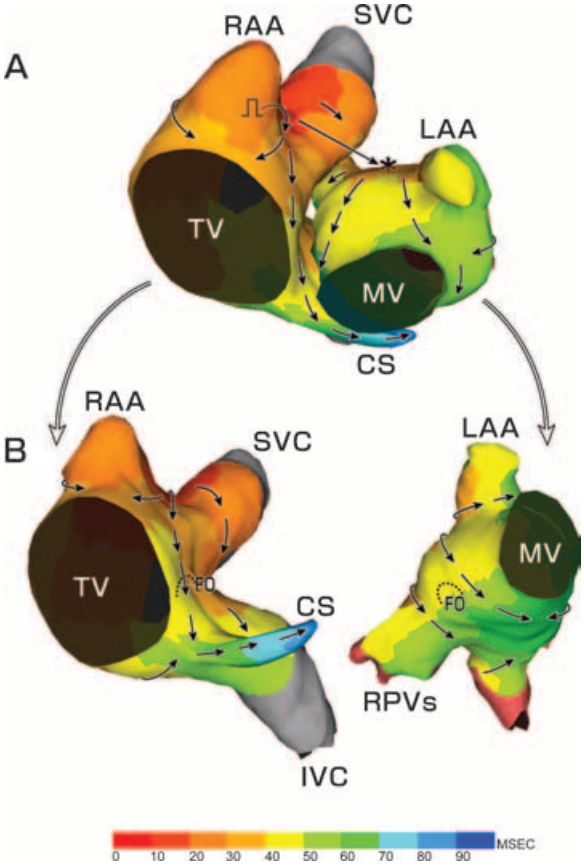

Figure 4. *Interatrial conduction and the atrial activation sequence during pacing from the HRA. A: The activation map is displayed on atrial molds viewed from the left anterior oblique and cranial projection. The rectangle indicates the site of stimulation. The activation time is depicted with 10 different color codes to represent each 10-msec period of activation. The paced activation conducted over Bachmann's bundle and the LA was activated from the superior septum indicated by the asterisk (*). The activation spread across the interatrial septum inferiorly. The activation on both sides of the septum is not fully observed in this view. B: The same activation map is displayed on the atrial split-molds in which the atrium is separated and rotated in the direction indicated by the open arrows in the figure in order to simultaneously observe the activation sequence of both sides of the septum. The semicircle dotted lines indicate the rim of fossa ovalis. The paced activation spread on the right-sided septum inferiorly while the left-sided septum was activated by the wavefront that originated from the earliest activation site in the superior LA septum indicated by the asterisk in the panel A. These wavefronts spread across the septum inferiorly along both sides of the septum concordantly. The CS was activated by the activation that propagated through the right-sided septum. The inferior LA was activated by the activation that propagated through the left-sided septum before the distal CS was activated. The following activation maps are displayed in both of these atrial molds. RAA = right atrial appendage; LAA = left atrial appendage; SVC = superior vena cave; IVC = inferior vena cave; TV = tricuspid valve; MV = mitral valve; CS = coronary sinus; RPVs = right pulmonary veins; and FO = fossa ovalis.*

postero-inferior septum of the LA, indicating a posterior septal connection as the single preferential connection.

During pacing from the LSPV, the earliest breakthrough in the RA appeared in the superior septum of the RA where the Bachmann's bundle was inserted in all animals. Meanwhile, the CS was activated in the left-to-right direction by the paced activation conducting over the LA–CS connection. However, the activation did not reach the ostium of the CS in any animal, because the activation collided in the CS with another activation that had conducted over Bachmann's bundle and propagated downward toward the right-sided interatrial septum (Fig. 6, left panel).

During pacing from the left inferior pulmonary vein, the CS musculature was the single preferential connection in two animals and Bachmann's bundle was the single preferential connection in four animals. In the remaining three animals, two distinct early breakthrough sites were identified simultaneously in the superior and inferior septa. The inferior septum was activated by the wavefront conducting through the CS musculature, while the superior septum was activated through Bachmann's bundle. These two wavefronts propagated to the RA septum superiorly and inferiorly, respectively, and collided with each other at the mid-portion of the septum (Fig. 6, right panel).

During pacing from the orifice of the RPVs, the earliest breakthrough was identified at the anterior-superior septum of the RA in three animals (anterior septal connection) and at the superior septum in two animals (Bachmann's bundle).

Interatrial Electrical Connections During Septal Pacing

The preference of the interatrial connections was variable during pacing from the septum. During pacing from the superior septum, Bachmann's bundle was the preferential interatrial connection, while the transseptal connections were the most preferential connections during pacing from the other septal sites (Fig. 3). During pacing from the mid-septum, the earliest breakthrough in the LA septum always appeared in the antero-superior septum, which was the site that was confirmed to be the opposite side of the limbus of the fossa ovalis by examination of the electrode location after each experiment. During pacing from the inferior septum, four of five animals exhibited two distinct interatrial connections simultaneously: the anterior septal connection and CS musculature. In one animal, only a single connection was observed in the CS musculature. During pacing from the posterior septum, the earliest breakthrough appeared in the posterior-inferior septum and in the anterior-superior septum of the LA simultaneously. The two wavefronts from the breakthrough sites collided with each other at the posterior septum of the LA. Although the stimulated activation propagated in the right-to-left direction in the CS, the activation conducting over the posterior septal connection activated the inferior wall of the LA in all animals. In two of three animals, the LA activation further conducted to the CS via the LA–CS connection. The activation propagated retrogradely toward the ostium of the CS and collided with the activation propagating directly from the pacing site (Fig. 7).

Conduction Properties of Interatrial Connections

The preference of the interatrial connections and pattern of activation in the contralateral atrium were consistent irrespective of the pacing cycle length. Figure 8 shows the activation time difference between the RA and LA across the four different interatrial connections as a function of the pacing cycle length. There was no significant decremental conduction in any of the connections.

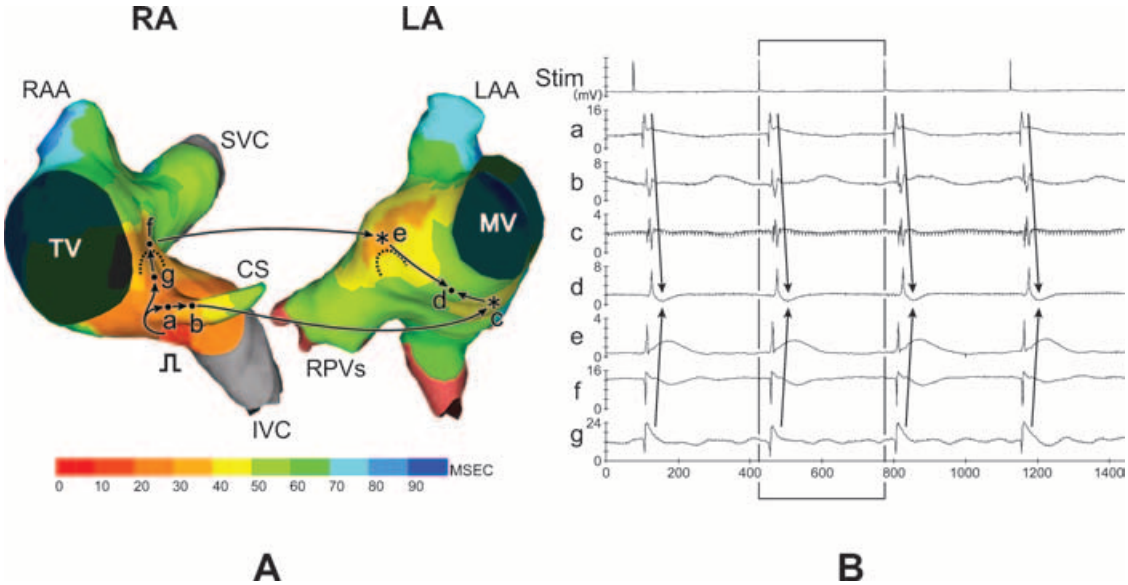

Figure 5. *Interatrial conduction and the atrial activation sequence during pacing from the LRA. A: Endocardial activation maps of both atria and the CS during pacing from the LRA at a pacing cycle length of 350 msec. B: Selected electrograms from both sides of the septum. Both atria are displayed in the split septal view. The activation map during the time window as indicated in panel B is shown. There were two components of the paced activation originating from the LRA. One component of the activation propagated superiorly over the lower RA septum, and subsequently conducted to the LA through the antero-superior septal connection (g–f–e). The other component of the activation propagated through the CS, and conducted to the LA over the coronary sinus musculature (a–b–c). The activation wavefronts of these two components collided with each other at the inferior LA (d). The figure symbols and legends of the maps are the same as in Figure 4.*

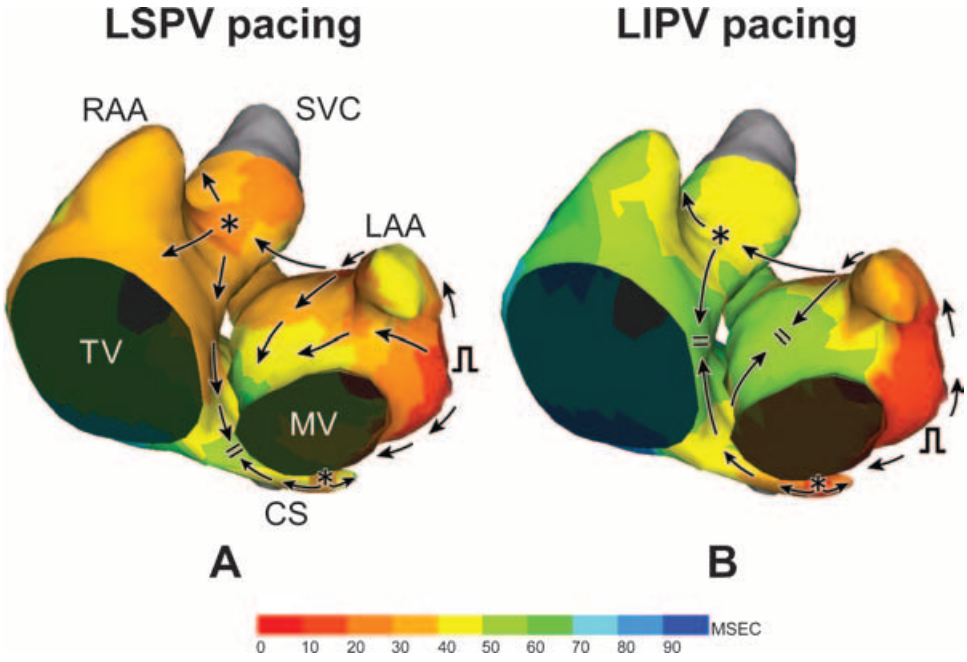

Figure 6. *Endocardial activation of the right and left atria during pacing from the LSPV (left panel) and LIPV (right panel) at a paced cycle length of 250 msec. The activation map represents the antero inferior view of both atria. During pacing from the LSPV, the activation conducted over Bachmann's bundle and activated the RA from the endocardium at the superior septum adjacent to the SVC (indicated by an asterisk). The activation spread inferiorly over both sides of the septum. The second earliest activation appeared at the mid-portion of the CS and propagated toward the distal CS and proximally toward the ostium of the CS. The activation collided with the other activation propagating over the right-sided septum in the CS. During pacing from the LIPV, two distinct early breakthrough sites were identified simultaneously in the RA septum in three out of nine animals. The earliest activation appeared at the superior septum as well as at the ostium of the CS. The wavefront from these two early activation sites collided with each other at the mid-septum of the RA. The figure symbols and legends of the maps are the same as in Figure 4.*

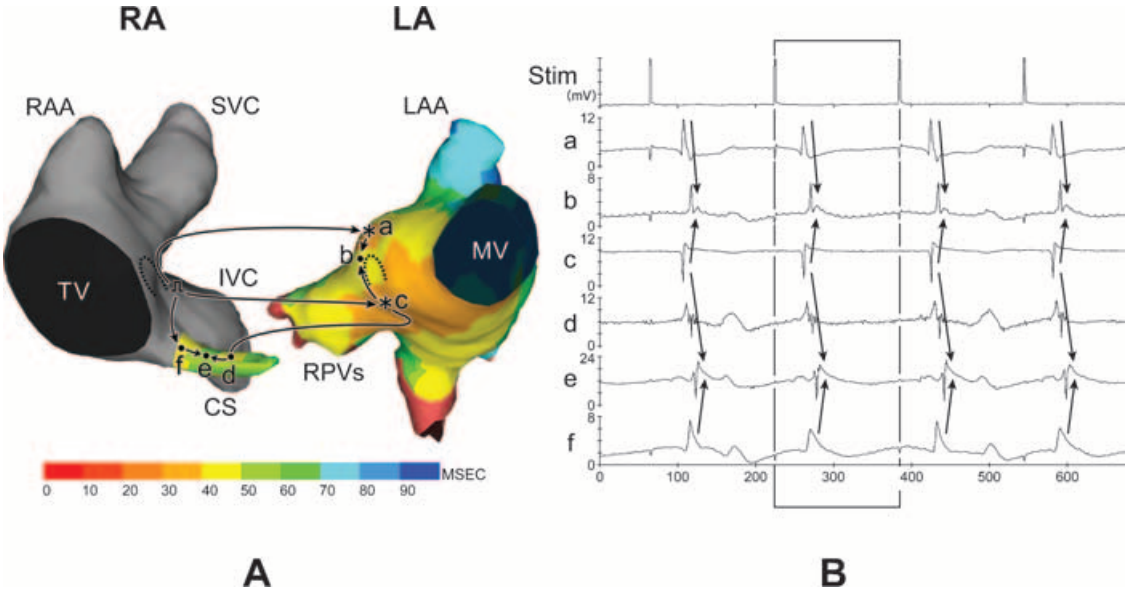

Figure 7. *Interatrial electrical connections during pacing from the posterior septum. A: Endocardial activation maps of both atria during pacing from the right-sided posterior septum at a pacing cycle length of 160 msec. B: Selected electrograms from the LA and CS. The location of the selected electrodes (a–f) is indicated in the maps. The other figure symbols are the same as in Figure 4. The RA endocardium was not mapped (gray area), because the electrode form was removed to facilitate pacing the right-sided septum. The earliest LA activation appeared at the antero-superior septum (a) and postero-inferior septum (c). These two activation wavefronts collided with each other at the mid-septum in the LA (b). The activation that appeared at the posterior septum propagated postero-medially and conducted over the LA–CS connection (d). The activation further propagated along the CS toward the ostium and collided in the CS (e) with the other wavefront that propagated directly from the site of pacing.*

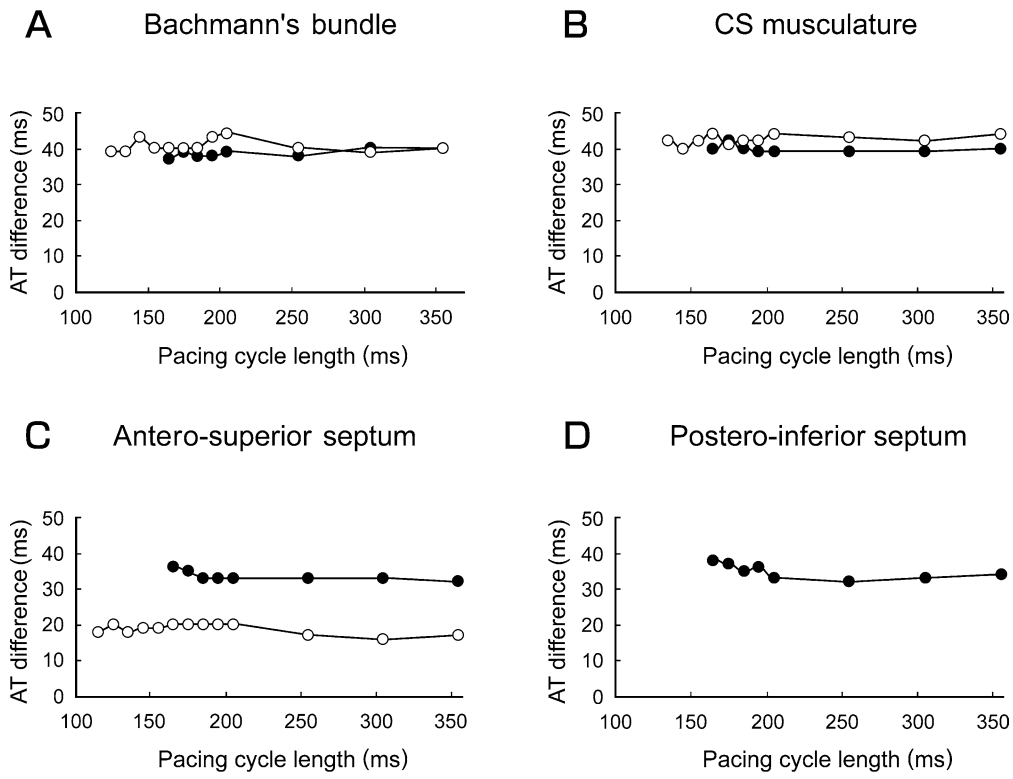

Figure 8. *Activation time difference across the interatrial connections. The activation time difference (AT difference) across Bachmann's bundle (A), CS musculature (B), antero-superior transseptal connection (C), and postero-inferior transeptal connection (D) was plotted as a function of the pacing cycle length. The open circles denote the difference during LA to RA conduction and the closed circles denote the difference during RA to LA conduction. Left to right conduction across the postero-inferior transeptal connection was not documented in the present study. No significant decremental conduction was demonstrated in any of the connections.*

Discussion

Location of the Transseptal Connections

In addition to Bachmann's bundle and the CS musculature, the interatrial electrical connections were identified at the antero-superior and postero-inferior septa in the present study. Although the RA has a large septal portion, the true extent of the septum is confined to the floor of the fossa ovalis and its antero-inferior rim.[11] In respect to the embryonic development of the atrial septum, there should be no interatrial connective tissue in the floor of the fossa ovalis. The antero-superior transseptal connection may be located in the anterior limbus of the fossa ovalis, which is not the septum, but a prominent muscular rim, constituting a septal component. Because one branch of Bachmann's bundle is contiguous to the limbus of the fossa ovalis,[12] the antero-superior transseptal connection could have been confused with the endocardial branch of Bachmann's bundle in the other studies. In the present study, the antero-superior septal connection was located at 3 to 6 interelectrode distances (9–18 mm) from the insertion of Bachmann's bundle, and was clearly differentiated from Bachmann's bundle by the activation sequence of the septum.

In contrast, it is unlikely that an actual transseptal connection exists in the posterior septum because both atrial walls are infolded and covered with an epicardial fat pad in the posterior septum.[13] The subepicardial band, which connects to the inferior wall of the LA and inferior cavo-atrial junction, might act as the interatrial electrical connection in the posterior septum.[14] The present mapping study showed that the earliest breakthrough of the posterior septal connection appeared in a relatively broad area in the postero-inferior septum of the LA, extending to the posterior LA where the CS–LA connection is located. The posterior septal connection could have been confused as the interatrial connection through the CS musculature in the other studies that used electrodes with low spatial resolution and without simultaneous recording of the electrograms in the CS.

Preference of Connections

All animals exhibited various patterns of preferential connections during pacing from the inferior atrial sites, whereas Bachmann's bundle was the single preferential connection during pacing from the superior atrial sites. All four electrical connections, including the transseptal connections, were demonstrated during pacing from the LRA, and Bachmann's bundle was never used as an interatrial connection during pacing from the mid-, inferior-, or posterior septum. These data suggest that the distance from the pacing site to the proximal end of each interatrial connection is the primary determinant for the preference of the interatrial connection.

In addition to the distance between the pacing site and the proximal end of the connection, the direction of the activation related to the myocardial architecture also determined the preference of the connection. Compared with the relatively homogeneous structure in the LA, the RA has a greater complexity of the myocardial architecture, such as the crista terminalis and pectinate muscles. As shown in Figure 2, Bachmann's bundle was the single preferential connection during pacing from the LRA in nearly half of the animals, even though the septal connections and the CS orifice were closer to the pacing site in the LRA. The stimulated wavefront conducted through the crista terminalis superiorly, reached the right-sided end of Bachmann's bundle, and activated the LA earlier than did the activation through the other connections. This phenomenon can be explained by the difference in the conduction velocity between the longitudinal and transverse propagation in inhomogeneous atrial tissue.[15] An inconsistent form of the branching of the crista terminalis may also explain the unique conduction properties in the LRA.[16]

Another example of the effect of the myocardial architecture on the preference of the connection was demonstrated in the activation maps during pacing from the inferior septum. The preferential connections for this pacing site were the anterior septal connection and CS musculature, and the connection through the posterior septum was not employed even though the site of the pacing was located adjacent to the connection. There are anatomical barriers such as the crista terminalis, Eustachian ridge, and tendon of Todaro in the inferior septum. These barriers could exhibit a conduction delay or block during pacing from the inferior septum.[17,18]

Role of Interatrial Connections in Atrial Tachyarrhythmias

The present study has suggested that a reciprocating reentrant activation between the RA and LA utilizing the interatrial connections can be a feasible electrophysiology mechanism in the perpetuation of atrial reentrant tachyarrhythmias. Interatrial macroreentry involving Bachmann's bundle and the CS musculature has been shown as a mechanism in the patients with atypical atrial flutter.[19] As shown in Figure 7, the CS was activated by the returning activation conducting through the LA–CS connection during pacing from the posterior RA septum. In diseased atria with nonuniform refractoriness and slow conduction, an unidirectional block can be induced and an interatrial reciprocating reentrant activation through the interatrial connections can be initiated.

Deen et al. have described that the activation map in the RA occurring during ectopic beats from each pulmonary vein is similar to that during pacing from the same pulmonary vein in patients with focal atrial fibrillation (AF).[20] The present study has demonstrated that Bachmann's bundle is the most preferential connection for activation originating from the RSPV or LSPV, and that it can be variable for activation originating from other atrial regions. The site of origin of the repetitive activation in the LA would govern the preferential connection and further determine the pattern of RA activation during focal AF.

Conduction Through the Interatrial Connections

All the interatrial connections exhibited one-to-one conduction without any conduction delay during pacing even with the shortest pacing cycle length that captured the atrium in the present study. Mansour et al. emphasized the role of the left to right activation rate gradient in the fibrillatory conduction of a focal LA activation to the RA in their acute AF model in sheep in the presence of acetylcholine.[21] We

also have previously demonstrated, in patients with permanent AF by intraoperative mapping, that a conduction delay or block in the propagation pathway of the LA repetitive activation to the RA is the mechanism for the concurrent multiple wavelets that are frequently seen in AF.[22] More recently, Sahadevan et al. demonstrated a decline in the dominant frequencies between the LA and RA and suggested that a rapid and regular driver in the LA causing fibrillatory conduction is one mechanism in chronic AF.[23] The reasons for the absence of conduction delay in the interatrial connections in the present study could be that we used normal canines and that, because of the refractoriness in the stimulation site or the atrial tissue proximal to the connection, the cycle length of the activation applied to the proximal end of the connection was not short enough to cause conduction delay within the connection. In the patients with persistent or permanent AF, electrical remodeling[24] due to a lasting rapid atrial activation may shorten the refractoriness and allow a more rapid activation. Nonuniform anisotropic characteristics imposed by long fibrotic strands have been shown to cause a progressive increase in the activation delay in chronically diseased myocardium.[25,26] These abnormalities would cause a significant conduction delay or block of the regional atrial activation and result in a complex and disorganized atrial activation during AF.

Limitations

The preferential connection was determined by the activation sequence of the contralateral atrium and the activations of the interatrial connections were not directly recorded except for the CS musculature. As shown in Figure 5, the conduction through the CS musculature was blocked at its ostium by the activation propagating through the other interatrial connection. This suggested that the conduction through the other connection could have been blocked within the connection, especially in the interatrial septal connections.

Moreover, the preference of the connections could have been determined anatomically, not by the conduction time difference between the different interatrial connections. Some animals could have lacked one of the connections congenitally. Surgical interruption of one of the connections and repeated mapping would be helpful in distinguishing these different mechanisms.[27]

Since this was an endocardial mapping study, the epicardial and endocardial difference in the conduction was not examined. Derakhchan et al.[10] mapped the atrial epicardium and endocardium simultaneously and described that the endocardial activation was faster than the epicardial activation in the RA, although the LA activation spread more symmetrically along the endocardial and epicardial surfaces. This intraatrial conduction property might have affected the preference of the interatrial connection during pacing from the RA.

Conclusion

Four distinct interatrial electrical connections were identified at the Bachmann's bundle, CS, and antero-superior and postero-inferior septa. The preference among the four interatrial electrical connections was determined by the site of activation and propagation of the activation related to the myocardial architecture. These unique preferential connections may play a significant role in the interatrial conduction and perpetuation of atrial tachyarrhythmias.

References

1. Bachmann G: The interauricular time interval. Am J Physiol 1916;41:309-320.
2. Dolber PC, Spach MS: Structure of canine Bachmann's bundle related to propagation of excitation. Am J Physiol 1989;257:H1446-H1457.
3. Ants M, Otomo K, Arruda M, Scherlag BJ, Pitha J, Tondo C, Lazzara R, Jackman WM: Electrical conduction between the right atrium and the left atrium via the musculature of the coronary sinus. Circulation 1998;98:1790-1795.
4. Chauvin M, Shah DC, Haissaguerre M, Marcellin L, Brechenmacher C: The anatomic basis of connections between the coronary sinus musculature and the left atrium in humans. Circulation 2000;101:647-652.
5. Ho SY, Sanchez-Quintana D, Cabrera JA, Anderson RH: Anatomy of the left atrium: Implications for radiofrequency ablation of atrial fibrillation. J Cardiovasc Electrophysiol 1999;10:1525-1533.
6. Roithinger FX, Cheng J, SippensGroenewegen A, Lee RJ, Saxon LA, Scheinman MM, Lesh MD: Use of electroanatomic mapping to delineate transseptal atrial conduction in humans. Circulation 1999;100:1791-1797.
7. Keith A, Flack M: The form and nature of the muscular connections between the primary divisions of the vertebrate heart. J Anat Physiol 1907;41:172-189.
8. Matsuo K, Uno K, Khrestian CM, Waldo AL: Conduction left-to-right and right-to-left across the crista terminalis. Am J Physiol Heart Circ Physiol 2001;280:H1683-H1691.
9. Sun H, Velipasaoglu EO, Wu DE, Kopelen HA, Zoghbi WA, Spencer III WH, Khoury DS: Simultaneous multisite mapping of the right and the left atrial septum in the canine intact beating heart. Circulation 1999;100:312-319.
10. Derakhchan K, Li D, Courtemanche M, Smith B, Broullette J, Page PL, Nattel S: Method for simultaneous epicardial and endocardial mapping of in vivo canine heart: Application to atrial conduction properties and arrhythmia mechanisms. J Cardiovasc Electrophysiol 2001;12:548-555.
11. Anderson RH, Brown NA, Webb S: Development and structure of the atrial septum. Heart 2002;88:104-110.
12. Lemery R, Guiraudon G, Veinot JP: Anatomic description of Bachmann's bundle and its relation to the atrial septum. Am J Cardiol 2003;91:1482-1485.
13. Ho SY, Anderson RH, Sanchez-Quintana D: Gross structure of the atriums: More than an anatomic curiosity? PACE 2002;25:342-350.
14. Ho SY, Anderson RH, Sanchez-Quintana D: Atrial structure and fibers: Morphologic bases of atrial conduction. Cardiovasc Res 2002;54:325-336.
15. Spach MS, Miller WT III, Dolber PC, Kootsey JM, Sommer JR, Mosher CE Jr: The functional role of structural complexities in the propagation of depolarization in the atrium of the dog. Cardiac conduction disturbances due to discontinuities of effective axial resistivity. Circ Res 1982;50:175-191.
16. Sanchez-Quintana D, Anderson RH, Cabrera JA, Climent V, Martin R, Farre J, Ho SY: The terminal crest: Morphological features relevant to electrophysiology. Heart 2002;88:406-411.
17. Betts TR, Ho SY, Sanchez-Quintana D, Roberts PR, Anderson RH, Morgan JM: Characteristics of right atrial activation during coronary sinus pacing. J Cardiovasc Electrophysiol 2002;13:794-800.
18. Sun H, Khoury DS: Electrical conduits within the inferior atrial region exhibit preferential roles in interatrial activation. J Electrocardiol 2001;34:1-14.
19. Olgin J, Jayachandran J, Engelstein E, Groh W, Zipes D: Atrial macroreentry involving the myocardium of the coronary sinus: A unique mechanism for atypical atrial flutter. J Cardiovasc Electrophysiol 1998;9:1094-1099.
20. Deen VR, Morton JB, Vohra JK, Kalman JM: Pulmonary vein paced activation sequence mapping: Comparison with activation sequences during onset of focal atrial fibrillation. J Cardiovasc Electrophysiol 2002;13:108-109.
21. Mansour M, Mandapati R, Berenfeld O, Chen J, Samie FH, Jalife J: Left-to-right of atrial frequencies during acute atrial fibrillation in the isolated sheep heart. Circulation 2001;103:2631-2636.
22. Nitta T, Ishii Y, Miyagi Y, Ohmori H, Sakamoto S, Tanaka S:

Concurrent multiple left atrial focal activations with fibrillatory conduction and right atrial focal or reentrant activation as the mechanism in atrial fibrillation. J Thorac Cardiovasc Surg 2004;127:770-778.
23. Sahadevan J, Ryu K, Peltz L, Khrestian CM, Stewart RW, Markowitz AH, Waldo AL: Epicardial mapping of chronic atrial fibrillation in patients. Circulation 2004;110:3293-3299.
24. Wijffels MC, Kirchhof CJ, Dorland R, Allessie MA: Atrial fibrillation begets atrial fibrillation. A study in awake chronically instrumented goats. Circulation 1995;92:1954-1968.
25. Li D, Fareh S, Leung TK, Nattel S: Promotion of atrial fibrillation by heart failure in dogs: Atrial remodeling of a different sort. Circulation 1999;100:87-95.
26. Kawara T, Derksen R, Groot JR, Coronel R, Tasseron S, Linnenbank AC, Hauer RNW, Kirkels H, Janse MJ, Bakker JMT: Activation delay after premature stimulation in chronically diseased human myocardium relates to the architecture of interstitial fibrosis. Circulation 2001;104:3069-3075.
27. Takayasu M, Tateishi Y, Osawa M: Experimental studies on the auricular flutter and fibrillation. Jpn Circ J 1958;21:477-483.

ACCURACY MATTERS

SEE THINGS DIFFERENTLY

With a first-of-its-kind, grid-patterned electrode configuration and HD wave bipole recordings along and across the splines, the Advisor™ HD Grid Mapping Catheter, Sensor Enabled™ gives you fast,[1] accurate[2] high-density cardiac maps. Experience both ease-of-use[3] and voltage recordings in direction independent mapping.[4]

Discover fast,[1] accurate[2] cardiac mapping with the Advisor HD Grid Mapping Catheter, Sensor Enabled.

Learn More at SJM.com/HDGrid

1. Abbott. Report on file. 90299533.
2. Abbott. Report on file. 90262900.
3. Abbott. Report on file. 90355919.
4. Abbott. Report on file. 90280703.

Abbott
One St. Jude Medical Dr., St. Paul, MN 55117 USA
Tel: 1 651 756 2000
SJM.com
St. Jude Medical is now Abbott.

Rx Only
Brief Summary: Prior to using these devices, please review the Instructions for Use for a complete listing of indications, contraindications, warnings, precautions, potential adverse events and directions for use.

28908-SJM-ADV-0818-0042 | Item approved for global use.

Abbott